química nova

Quim. Nova **2026**, *49*, e-20260042, 1-7
http://dx.doi.org/10.21577/0100-4042.20260042

Article

KERATIN EXTRACTION FROM POULTRY WASTE AND ASSESSMENT OF ITS ANTIBACTERIAL ACTIVITY AGAINST *Staphylococcus aureus*

Fabricio S. Vargas[a], Marco C. Chavez[a], Faiz Ahmed[b,*], Elizabeth C. Pastrana[a,*] and Roxana Y. Pastrana-Alta[a,*]
[a]Laboratory Biomet, School of Chemistry, Universidad Nacional de Ingeniería, 15311 Lima, Perú
[b]Department of Chemistry, Government College University Faisalabad, New Campus Jang Road, 38000 Punjab, Pakistan

Received: 10/30/2025; accepted: 02/19/2026; published online: 03/12/2026

Feathers from poultry waste, composed of approximately 90% keratin, represent an environmental burden but also a valuable source of biopolymers. This study assessed keratin extraction via a chemical reduction method. Two protocols were used: Ke-1, employing urea and sodium sulfite at pH 7 under reflux at 75 °C for 10 h, and Ke-2, which incorporated sodium dodecyl sulfate (SDS) at pH 9 for 4 h. After dialysis and lyophilization, the yields were 70% (Ke-1) and 78% (Ke-2). Fourier transform infrared spectroscopy (FTIR) spectra showed characteristic bands (amide A, I, II, III), confirming α-helix and β-sheet secondary structures. X-ray diffraction (XRD) analysis exhibited peaks at 19.03° (Ke-1) and 19.51° (Ke-2), indicating the predominance of β-sheets. Thermogravimetric analysis (TGA) revealed two thermal events: dehydration near 100 °C and degradation of the α and β structures of keratin between 240-400 °C. Micrographs obtained by scanning electron microscopy (SEM) indicated fibrillar morphology with hollow cavities, with Ke-2 displaying larger fiber diameters. The ^{1}H nuclear magnetic ressonance (NMR) spectrum confirmed signals from amino, carboxyl, methyl, and methylene groups, associated with amino acid residues of keratin. Notably, Ke-2 exhibited dose-dependent bacteriostatic activity against *Staphylococcus aureus*. This study demonstrates the valorization and reuse of organic residues derived from the poultry industry through an efficient and scalable processing method for converting poultry waste into high-value keratin with promising biomedical and antimicrobial applications.

Keywords: keratin; extraction; chemical reduction; α- and β-structure; circular chemistry.

INTRODUCTION

Global poultry meat production increased from 9 to 133 million tons between 1961 and 2020, with poultry accounting for nearly 40% of total global meat production by the end of that period.[1] It is estimated that poultry farming generates more than 5 million tons of feather waste annually worldwide.[2] In South America and globally, poultry production continues to rise.[3] In 2019, global poultry meat production reached 100.8 million tons, representing a 1.5% increase over the previous year. In Peru, chicken production has grown notably by 7% over the last decade.[3] This increase in production and consumption has led to an accumulation of approximately 8.5 billion tons of feathers annually, derived from the slaughter of around 24 billion chickens.[2] Improper disposal of these residues contributes significantly to environmental pollution, particularly when deposited directly into soil or water bodies.[4] For instance, incineration, the primary disposal method, requires high energy input and emits large amounts of black carbon and carbon dioxide.[5,6]

However, poultry industry residues, particularly feathers, should not be regarded as waste without intrinsic value.[7] Feathers are composed of approximately 90% keratin, an insoluble, fibrous, and highly resilient protein.[8-10] Keratin can be utilized in various applications such as films, hydrogels, biofertilizers, and biosorbents.[11] Keratin is rich in cysteine residues (7-13%) within its amino acid sequence.[12] These cysteine residues can form disulfide bonds, both inter- and intramolecular, resulting in a highly crosslinked polypeptide. This network provides thermal stability, high mechanical strength, hydrophobicity, and excellent solid-state stability.[13] There are two main types of keratin: α-keratin, found in wool, hair, nails, and skin; and β-keratin, present in spider silk, feathers, claws, and bird beaks.[14] α-Keratin is distinguished by its high content of disulfide bridges, which confer mechanical robustness.[9] The insolubility of keratin in common solvents is mainly due to these disulfide bonds. Therefore, the disruption of disulfide linkages is essential for solubilizing keratin, particularly when extracting it from feathers.[14] Several extraction methods have been explored, including alkaline hydrolysis, sulfitolysis, ionic liquid extraction, oxidative treatment, supercritical water extraction, and steam explosion.[15,16] Among these, chemical reduction is one of the most effective and widely adopted techniques due to its rapid reaction kinetics.[15,16] During the reduction process, soluble keratins are formed, containing non-degraded amino acids. Sulfitolysis plays a central role in this process.[17] In sulfitolysis, disulfide bonds are cleaved by sulfite ions, resulting in cysteine thiols (reduced keratin) and cysteine-*S*-sulfonate residues (Bunte salts).[15] Disulfide bonds can be disrupted using reducing agents such as dimethyl sulfoxide (DMSO), thioglycolic acid, sodium sulfide, or 2-mercaptoethanol.[18] These reactions are typically performed in the presence of a denaturing agent like urea[19] and a surfactant such as sodium dodecyl sulfate (SDS).[18] At pH levels above 9, sulfitolysis becomes reversible; hence, denaturing agents help prevent reformation of disulfide bridges.[20]

Antimicrobial peptides (AMPs) derived from natural proteins such as keratin have garnered attention as potential alternatives to traditional antibiotics. Thus, keratin can disrupt the microbial balance and promote resistance.[21] These peptides interact with bacterial membranes, compromising their integrity and exhibiting bacteriostatic effects. The cysteine-rich structure of keratin facilitates membrane interaction through disulfide-mediated stabilization.[22] Additionally, keratin contains bioactive tripeptides like Arg-Gly-Asp and Leu-Asp-Val, which are associated with cell adhesion processes.[23]

*e-mail: rpastranaa@uni.edu.pe
Associate Editor handled this article: Fernanda G. Finelli

Recent studies have demonstrated the significant antibacterial activity of keratin against several pathogens. For instance, Majeed *et al.*[24] reported that keratin extracted from porcupine produced inhibition zones of 16.5 ± 0.71 mm against *Escherichia coli* and 15.75 ± 0.35 mm against *Staphylococcus aureus*. Furthermore, keratin nanoparticles combined with lipids exhibited even greater inhibition, 3.50 ± 0.70 mm for *E. coli* and 25.75 ± 0.35 mm for *S. aureus*. These findings suggest that keratin and its derivatives represent an effective and sustainable alternative for the development of new antimicrobial agents.

This study aimed to evaluate keratin extraction from duck feathers generated by the poultry industry using two simple and efficient chemical reduction-based methods (Ke-1 and Ke-2). The extracted keratin was thoroughly characterized. In addition, antibacterial activity was assessed through inhibition zone assays against *S. aureus*, confirming a concentration-dependent increase in antibacterial efficacy.

EXPERIMENTAL

Materials

Feathers were disinfected with 96% ethanol (Hersil). Degreasing was performed using 90% petroleum ether (Merck). Keratin extraction employed urea (99.5 mol%, Merck), sodium sulfite (98%, Merck), and sodium dodecyl sulfate (SDS, 99%, Sigma-Aldrich). Dialysis was carried out with a membrane of molecular-weight cut-off > 14 kDa (Sigma-Aldrich). Luria-Bertani (LB) broth and bacteriological-grade agar were obtained from HiMedia (BioGenics, Peru). *Staphylococcus aureus* ATCC 29213 was provided by Microbiologics (Peru) and stored at 4 °C.

Feather preparation

The feathers were initially washed in stages using running water at 40 °C and a cleansing agent to remove foreign materials (e.g., sticks, stones, tissue remnants). They were then immersed in a 70% ethanol-ultrapure water solution (70:30 v/v), filtered, drained, and dried in an oven at 30 °C for 24 h. Degreasing was performed using a Soxhlet extractor with 100 mL of petroleum ether for 6 h. The excess solvent was filtered off, and the feathers were oven-dried at 40 °C for 24 h. The dried feathers were subsequently ground and stored at room temperature until used for keratin extraction.

Keratin extraction from conditioned feathers

Keratin extraction was performed following two different protocols.[25] For Ke-1 synthesis, a solution containing urea (6 mol L^{-1}) and sodium sulfite (0.5 mol L^{-1}) was prepared, adjusted to pH 7. For Ke-2 synthesis, the solution included urea (6 mol L^{-1}), sodium sulfite (0.5 mol L^{-1}), and SDS (0.2 mol L^{-1}), adjusted to pH 9 using HCl. Both solutions were mixed with prepared feathers at a ratio of 1:25 (m/v). Extraction was conducted under reflux at 75 °C with continuous stirring. The extraction time was selected based on previously reported studies in which the sulfitolysis process was conducted over a range of 2 h[26] to 6 h.[27] In the present work, two significantly different extraction times (4 and 8 h) were chosen to evaluate their effect on the process. The resulting mixtures were purified via dialysis with continuous agitation and water changes every 5 h for a total of 50 h. The dialyzed solutions were centrifuged (5000 rpm, 15 min, room temperature) to remove residual impurities, frozen at –70 °C for 5 h, and then freeze-dried for 72 h. The resulting keratins, designated Ke-1 and Ke-2, were stored at –20 °C until characterization.

Evaluation of bacteriostatic activity against *Staphylococcus aureus*

Bacterial culture

S. aureus (ATCC 29213) was cultured and stored on Luria-Bertani (LB) agar (composed of 10 g tryptone, 5 g yeast extract, and 5 g NaCl in 1 L of deionized water) at 4 °C for the performance of the assays. Visual turbidity of the culture tubes was recorded before and after incubation. Mueller-Hinton agar was used as the solid culture medium. For the antibacterial assays, stored *S. aureus* cultures were incubated overnight at 37 °C in LB broth. Culture turbidity was adjusted by spectrophotometry to an optical density of 0.10 at 625 nm (corresponding to 10^8 colony forming unit (CFU) mL^{-1}, equivalent to McFarland standard 0.5), and CFUs were confirmed using plate counting methods.

Disk diffusion assay

The bacteriostatic activity of the keratin solutions was evaluated qualitatively using the disk diffusion method against *S. aureus*. Each concentration was tested in triplicate. Filter paper disks were loaded with keratin solutions at four concentrations: 12.5, 25.0, 50.0, and 100.0 mg mL^{-1}. The bacterial inoculum was spread on Mueller-Hinton agar, followed by the placement of the keratin-loaded disks. The plates were incubated at 37 °C for 24 h. The diameter of the inhibition zone was measured using a Vernier caliper.

Protein extraction yield

The extraction yield was calculated based on the dry weight of lyophilized keratin in relation to the initial weight of processed feathers, as described by Equation 1:

$$\text{Extraction yield (\%)} = \frac{W'}{W} \times 100\ \% \quad (1)$$

where W' is the weight of the lyophilized sample and W is the initial weight of the feathers.

Characterization

Fourier transform infrared spectroscopy (FTIR)

The obtained samples were characterized using FTIR with an IR Prestige-21 spectrometer (Shimadzu, Japan). Spectra were recorded in the wavenumber range of 550 to 4000 cm^{-1} with a resolution of 4 cm^{-1}. The data were processed using Origin 8.0 (OriginLab Corporation, Northampton, USA).

Thermogravimetric analysis (TGA)

Thermal stability analysis was carried out using an STA 6000 simultaneous thermal analyzer (PerkinElmer, USA) under standard conditions.

X-ray diffraction (XRD)

X-ray diffraction measurements were conducted using a MiniFlex 600 diffractometer (Rigaku, Japan) equipped with a Cu Kα radiation source (40 kV, 30 mA, λ = 1.5418 Å). Diffraction patterns were recorded over the 2θ range from 0° to 70°.

Scanning electron microscope (SEM)

The morphological features of the keratin samples were examined using a scanning electron microscope (JEOL 7500F, Japan). Images were captured to analyze surface structure and fiber morphology.

Proton nuclear magnetic resonance spectroscopy (^{1}H NMR)

^{1}H NMR spectra were recorded at the analytical center using a Bruker Avance Ascend AVIII HD 800 MHz spectrometer (Germany). D_2O was used as the solvent for all keratin samples.

Bacteriostatic characterization

The bacteriostatic activity of keratin was qualitatively assessed using the disk diffusion method on standardized filter paper disks.[28] The gram-positive strain *Staphylococcus aureus* ATCC 29213 was previously cultured in Luria-Bertani (LB) broth at 37 °C for 12 h until a turbidity corresponding to McFarland standard 0.5 was achieved. The microorganism was inoculated by streaking onto nutrient agar plates. After 20 min, four filter paper disks (1 mm thick, 6 mm diameter) were placed on the agar surface. Each disk was impregnated with 20 µL of keratin solution at concentrations of 12.5, 25.0, 50.0, and 100.0 mg mL^{-1}. Plates were incubated at 37 °C for 24 h. Antibacterial activity was determined by measuring the diameter of the inhibition zone (IZD), in millimeters, using a digital precision caliper.

RESULTS AND DISCUSSION

Fourier transform infrared spectroscopy (FTIR)

To analyze the structural features of the extracted keratins (designated Ke-1 and Ke-2), FTIR measurements were performed as shown in Figure 1. The spectra of both samples displayed similar profiles and revealed characteristic absorption bands corresponding to amide A, amide I, amide II, and amide III, which provide insights into the secondary structure of keratin.[29]

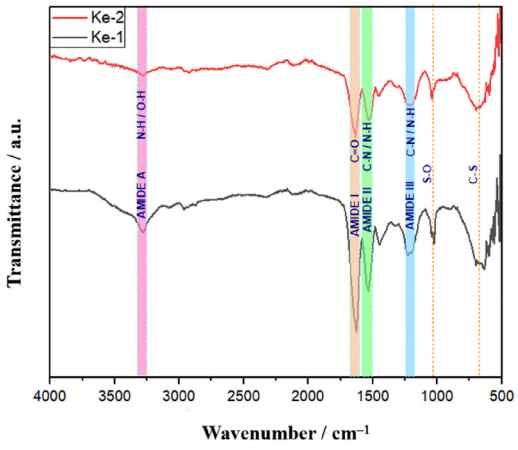

Figure 1. *FTIR spectra of keratins Ke-1 and Ke-2 extracted from duck feathers*

The amide A band, associated with N–H and O–H stretching vibrations, was observed only in Ke-1 at 3283 cm^{-1}.[16,30] This band is also linked to the α-helix conformation of the keratin secondary structure.[31] The amide I band, attributed to C=O stretching, appeared at 1641 cm^{-1} in Ke-1 and 1643 cm^{-1} in Ke-2, confirming the presence of protein backbone vibrations.[18,27] The amide II band, arising from C–H stretching and N–H bending, was located at 1535 cm^{-1} for Ke-1 and 1531 cm^{-1} for Ke-2.[16,32] Additionally, the amide III band, corresponding to the in-phase combination of C–N stretching and N–H bending, was detected at 1231 cm^{-1} in Ke-1 and 1230 cm^{-1} in Ke-2.[18,33] The presence of amide I, II, and III bands is indicative of β-sheet secondary structures in the keratin samples.[34]

Although the overall spectral patterns of Ke-1 and Ke-2 were similar, the intensity of the peaks was higher in Ke-1. This difference in intensity suggest a better concentration of characteristic keratin bonds in Ke-1 compared to Ke-2. Moreover, bands at 1024 (Ke-1) and 1041 cm^{-1} (Ke-2) were associated with S–O stretching vibrations of Bunte salt (cysteine-*S*-sulfonate) groups, which are generated during the sulfitolysis process and remain in the final product.[35,36] Additional peaks at 692 cm^{-1} in Ke-1 and 690 cm^{-1} in Ke-2 correspond to C–S bond stretching, a typical vibrational mode of keratin.[37]

Thermogravimetric analysis (TGA)

The thermogravimetric curves of the extracted keratins Ke-1 and Ke-2 are shown in Figure 2. Both keratins exhibited two distinct stages of thermal decomposition. The first stage occurred near 100 °C and was attributed to sample dehydration, with a weight loss of 6.73% for Ke-1 and 5.70% for Ke-2.[38] The second major weight loss, observed between 240 and 400 °C, corresponds primarily to the breakdown of disulfide bonds and the decomposition of secondary α-helix and β-sheet structures, as well as polypeptide chains.[39-41] Additionally, volatile compounds such as SO_2 and H_2S were released due to disulfide bond cleavage, typically occurring between 230 and 250 °C.[42] The pyrolysis of keratin, which begins around 150 °C, leads to the formation of various nitrogen- and sulfur-containing compounds derived from the thermal degradation of amino acids present in the keratin structure.[43]

As seen in Figure 2, the TGA profiles of both samples show a high degree of similarity, which is consistent with their common origin (duck feathers). However, the slight difference in total mass loss may be attributed to the different extraction methodologies, with Ke-1 likely containing a greater number of intramolecular disulfide bonds compared to Ke-2.[44]

This observation is also supported by the higher IR peak intensities observed in Figure 1 for Ke-1. Finally, the total weight loss was 92.25% for Ke-1 and 91.19% for Ke-2, indicating comparable thermal decomposition behavior. Table 1 summarizes the decomposition stages, temperature ranges, and corresponding weight loss percentages.

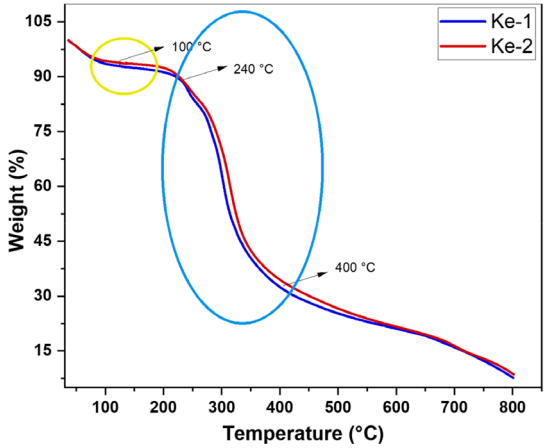

Figure 2. *TGA of keratins Ke-1 and Ke-2 extracted from duck feathers*

Table 1. Decomposition stages and associated weight loss for Ke-1 and Ke-2

Temperature / °C	Weigth loss / %		Degradation event
	Ke-1	Ke-2	
ca. 100	6.47	5.70	dehydration
240-400	54.41	53.17	β-keratin, S–S bonds and polypeptides
230-250	4.85	3.87	release SO_2 and H_2S
400-800	24.74	25.69	carbonaceous residues

X-ray diffraction (XRD)

X-ray diffraction (XRD) analysis was carried out to determine the crystalline phases of the keratin samples, as shown in Figure 3. Two diffraction peaks were observed in the 2θ profiles of Ke-1 and Ke-2. The first peak, located at 9.7° for Ke-1 and 9.9° for Ke-2, corresponds to the α-helix structural pattern.[45,46] The second peak, found at 19.2° and 19.5° for Ke-1 and Ke-2, respectively, is associated with the β-sheet structure.[47,48]

The intensity of the second peak reflects the relative abundance of β-sheet conformations in both samples, which were more prominent than α-helices.[49]

Moreover, the diffraction peak at 19.5° in Ke-2 was broader than that of Ke-1, suggesting increased overlap and disorder within the β-sheet domains.[50] This broadening can be attributed to the presence of SDS, which induces structural changes in the protein by disrupting intramolecular bonds, thereby reducing intrachain recombination and promoting the formation of intermolecular linkages.[51] Such rearrangement in protein structure, caused by SDS interactions, leads to a decrease in structural order in Ke-2, as evidenced by the broader XRD peak compared to Ke-1.[51,52]

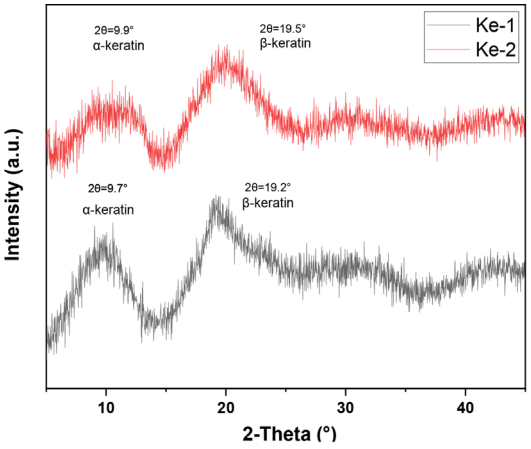

Figure 3. *XRD patterns of keratins Ke-1 and Ke-2 extracted from duck feathers*

Scanning electron microscopy (SEM)

The morphological characterization of the extracted keratins, Ke-1 and Ke-2, was carried out using SEM, as illustrated in Figure 4. The SEM images revealed a clearly defined fibrillar structure with distinct hollow internal cavities, where multiple fibers were observed to interweave.[53,54]

To precisely determine fiber diameters, a Gaussian fitting analysis was performed. The results showed that Ke-1 fibers had an average diameter of approximately 404 ± 174 nm (Figure 4a), while Ke-2 fibers exhibited a significantly larger average diameter of 595 ± 186 nm (Figure 4b). This increase in fiber diameter in Ke-2 is attributed to the presence of SDS in the extraction system. During dialysis, SDS interacts with keratin to form a complex through electrostatic interactions between the sulfate anion and positively charged side chains, as well as hydrophobic interactions between the dodecyl tail of SDS and nonpolar regions on the keratin surface adjacent to cationic sites.[52]

These interactions contribute to the enlargement of the keratin fiber diameter. Moreover, SDS acts as an effective inhibitor of cysteine oxidation when in its reduced state, thereby preventing the reformation of intramolecular disulfide bonds.[55] This suppression of intrachain recombination promotes the formation of intermolecular disulfide bridges between keratin molecules, leading to fiber aggregation and the formation of larger keratin-SDS complexes.[52] Due to the larger fiber diameter in Ke-2 (Figure 4b), this sample may also exhibit increased angular dispersion in X-ray diffraction patterns, as observed in Figure 3.

Although trace amounts of SDS do not significantly interfere with the keratin extraction efficiency from duck feathers, it is important to consider its implications for pharmaceutical or food-related applications. SDS lacks regulatory approval for ingestion and may pose safety risks due to its potential to cause skin and eye irritation.[54,56] Nevertheless, keratin-based films and hydrogels obtained using SDS have demonstrated effectiveness in *in vitro* drug delivery systems.[57,58] Similarly, keratin has shown significant utility in biomedical applications, including as a hemostatic agent and in the prevention of infections in open wounds.[59]

Proton nuclear magnetic resonance spectroscopy (^{1}H NMR)

The ^{1}H NMR spectrum of Ke-2 is shown in Figure 5. The signal corresponding to the free amino group (–NH_2) of amino acids was detected at 8.61 ppm, while amide NH protons were observed in the range of 7.35-6.84 ppm.[60] Free hydroxyl groups (–CH_2OH), characteristic of serine-like units, appeared in the range of 4.84-4.70 ppm. Geminal cyclic –CH_2 protons were detected at 3.92 ppm.[61] β-Protons adjacent to carboxylic acid groups (–COOH) were observed in the 3.2-3.7 ppm region.[62] Signals at 2.02 ppm were attributed to cyclic amines, while additional geminal cyclic –CH_2 signals were detected between 1.93 and 1.63 ppm.

Signals attributed to –CH_2 groups of valine- and leucine-like aliphatic chains were found between 1.49 and 1.18 ppm. Methyl groups (–CH_3) appeared between 0.95 and 0.84 ppm, and other cyclic geminal protons were detected at 0.89, 0.87, 0.84, 0.16, and 0.07 ppm.

Antibacterial activity of keratin at different concentrations against pathogen *S. aureus*

The antibacterial properties of keratin are well documented in the literature. In this context, we chose to confirm this relevant behavior using one representative extracted keratin sample. The Ke-2 sample, which exhibited the lowest characteristic signals among the keratin samples obtained, was therefore selected as an appropriate candidate for antibacterial evaluation. Under the assumption that Ke-1, showing superior keratin characteristics, would exhibit equal or enhanced antibacterial performance.

The bacteriostatic activity of keratin was evaluated against *S. aureus*. The inhibition zone diameters (IZD) formed by different concentrations of Ke-2 keratin against *S. aureus* are shown in Figure 6 and summarized in Table 2. A progressive increase in inhibition zone diameter was observed as the keratin concentration increased. This effect can be attributed to keratin-derived peptides interacting with lipoteichoic acid present in the membranes of gram-positive bacteria, leading to disruption of cellular structure and inhibition of bacterial proliferation.[63]

At a concentration of 100 mg mL^{-1}, the inhibition zone reached a maximum of 11.95 ± 2.7 mm, while at 12.5 mg mL^{-1}, it significantly decreased to 7.21 ± 0.76 mm.

Although sodium dodecyl sulfate (SDS) is known to exhibit antibacterial activity by disrupting cell membranes and denaturing proteins,[64] the presence of residual SDS in the Ke-2 samples is unlikely due to thorough purification by dialysis. However, a low possibility of residual SDS cannot be entirely excluded and should be considered prior to confirmation using quantitative analytical methods.

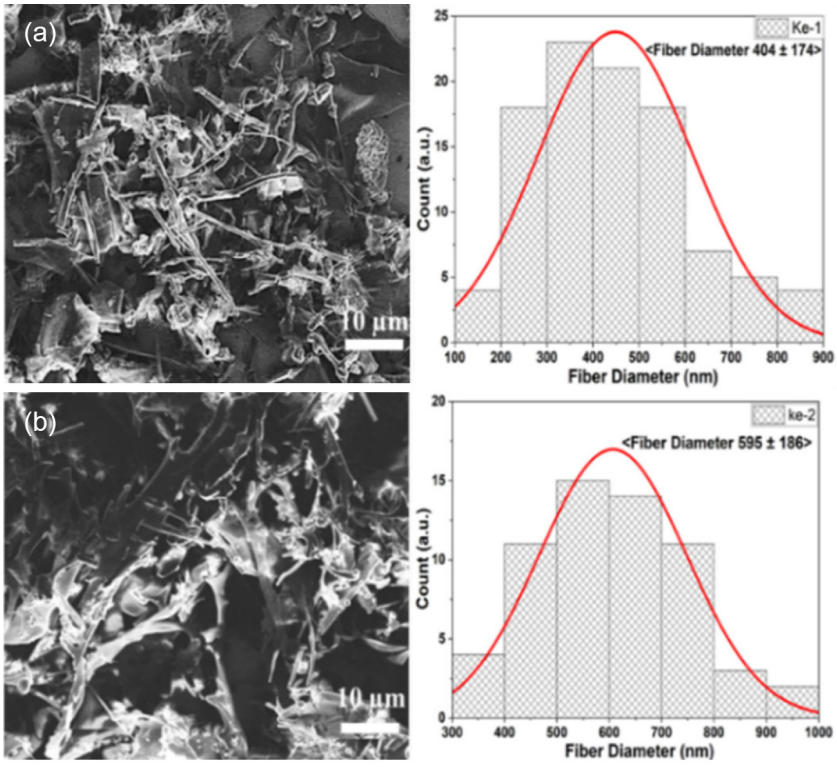

Figure 4. *SEM images of keratin morphology and fiber diameter for Ke-1 (a) and Ke-2 (b) extracted from duck feathers*

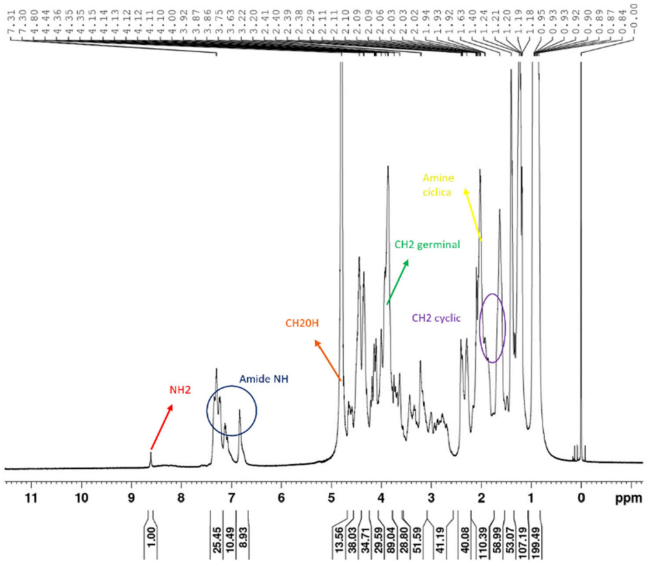

Figure 5. *^{1}H NMR spectrum of extracted keratin (Ke-2) recorded at 25 °C*

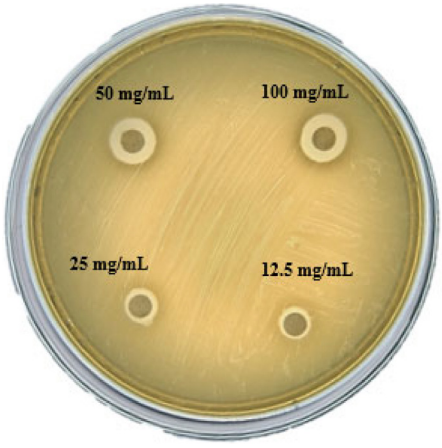

Figure 6. *Diameter of the inhibition zone of S. aureus after exposure to Ke-2 at different concentrations (12.5, 25, 50, and 10 mg mL^{-1})*

Table 2. Inhibition zone diameter of *Staphylococcus aureus* exposed to Ke-2 keratin at various concentrations

Ke-2 concentration / (mg mL^{-1})	IZD / mm
100	11.95 ± 2.71
50	10.02 ± 0.34
25	9.61 ± 3.42
12.5	7.21 ± 0.76

IZD: inhibition zone diameter.

CONCLUSIONS

Keratin was successfully extracted using two chemical reduction-based methods (Ke-1 and Ke-2), employing low-toxicity reagents with minimal environmental impact. The yields obtained were 70% for Ke-1 and 78% for Ke-2, the latter involving SDS in the extraction process.

Spectroscopic characterizations confirmed the presence of both α-helix and β-sheet secondary structures in the extracted keratins. The predominance of the β-sheet conformation is consistent with the avian feather origin of the protein. FTIR and ^{1}H NMR analyses showed prominent peaks in specific regions, indicating the presence of functional groups associated with constituent amino acids, such as amide I, II, and III bands, amino groups (–NH_2), carboxyl groups (–COOH), among others. Morphological characterization revealed a fibrillar structure with hollow cavities in both keratin products. Notably, Ke-2 exhibited a larger fiber diameter; however, this did not adversely affect thermal stability, as both extracted keratin samples demonstrated comparable thermal stability according to the TGA results.

Importantly, the keratin obtained via the Ke-2 method exhibited antibacterial activity against *Staphylococcus aureus*, with a clear dose-response relationship. This biological effect is attributed to keratin-derived peptides that potentially disrupt the bacterial cell wall, offering a natural alternative to conventional antimicrobials.

This study confirms the effective extraction of two types of keratin (Ke-1 and Ke-2) from poultry waste using a simple, efficient, and cost-effective chemical reduction method. These findings highlight the potential of the extracted keratins for applications in biomedical, pharmaceutical, and environmental fields.

DATA AVAILABILITY STATEMENT

The data set is available at https://doi.org/10.5281/zenodo.17479753.

ACKNOWLEDGMENTS

The authors thank UNI (project VRI-UNI FC-PFE-01-2023) for financial support; the BIOMET laboratory for workspace, materials, and reagents; the GISMA laboratory for additional reagents; Dr. Clemente L. Caycho and Dr. Pierre R. Apestegui for SEM technical assistance; and Mrs. Irma C. Acuña for supplying feathers for keratin extraction.

REFERENCES

1. Rofner, N. F.; *Revista de Investigaciones Altoandinas* **2019**, *21*, 225. [Crossref]
2. Paolilli, M. C.; Iglesias, B. F.; Cabrini, S. M.; Fillat, F. A.; Pagliaricci, L. O.; *La Cadena de Carne Aviar en Argentina*; INTA-EEA Pergamino: Argentina, 2021. [Link] accessed in March 2026
3. Husain, M. S. B.; Gupta, A.; Alashwal, B. Y.; Sharma, S.; *Energy Sources, Part A* **2018**, *40*, 2388. [Crossref]
4. Ferrareze, P. A. G.; Correa, A. P. F.; Brandelli, A.; *Biocatal. Agric. Biotechnol.* **2016**, *7*, 102. [Crossref]
5. Maurya, S. D.; Singh, A.; *Sustainable Chem. Eng.* **2023**, *5*, 31. [Crossref]
6. Dutta, H.; Bora, D.; Chetia, P.; Bharadwaj, C.; Purbey, R.; Bohra, R. C.; Dutta, K.; Rajulu, A. V.; Sadiku, E. R.; Selvam, S. P.; Gurusamy, P.; Rawal, R. K. J.; *Renewable Sustainable Energy Rev.* **2024**, *197*, 114394. [Crossref]
7. Maciel, J. L.; Werlang, P. O.; Daroit, D. J.; Brandelli, A.; *Waste Biomass Valorization* **2017**, *8*, 1177. [Crossref]
8. Kamarudin, N. B.; Sharma, S.; Gupta, A.; Kee, C. G.; Chik, S. M. S. B. T.; Gupta, R.; *3 Biotech* **2017**, *7*, 127. [Crossref]
9. Reddy, N.; Yang, Y.; *J. Polym. Environ.* **2007**, *15*, 81. [Crossref]
10. Nuutinen, E. M.; Willberg-Keyriläinen, P.; Virtanen, T.; Mija, A.; Kuutti, L.; Lantto, R.; Jääskeläinen, A. S.; *RSC Adv.* **2019**, *9*, 19720. [Crossref]
11. Chilakamarry, C. R.; Mahmood, S.; Saffe, S. N. B. M.; Arifin, M. A. B.; Gupta, A.; Sikkandar, M. Y.; Begum, S. S.; Narasaiah, B.; *3 Biotech* **2021**, *11*, 220. [Crossref]
12. Fagbemi, O. D.; Sithole, B.; Tesfaye, T.; *Sustainable Chem. Pharm.* **2020**, *17*, 100267. [Crossref]
13. Dou, Y.; Huang, X.; Zhang, B.; He, M.; Yin, G.; Cui, Y.; *RSC Adv.* **2015**, *5*, 27168. [Crossref]
14. Wang, Y. X.; Cao, X. J.; *Process Biochem.* **2012**, *47*, 896. [Crossref]
15. Khumalo, M.; Sithole, B.; Tesfaye, T. J.; *Environ. Manage.* **2020**, *262*, 110329. [Crossref]
16. Badrulzaman, S. Z. S.; Aminan, A. W.; Ramli, A. N. M.; Man, R. C.; Azelee, N. I. W.; *Mater. Sci. Forum* **2021**, *1025*, 157. [Crossref]
17. Pourjavaheri, F. S.; Pour, S. O.; Jones, O. A.; Smooker, P. M.; Brkljača, R.; Sherkat, F.; Shanks, R. A.; *Process Biochem.* **2019**, *82*, 205. [Crossref]
18. Alahyaribeik, S.; Ullah, A.; *Int. J. Biol. Macromol.* **2020**, *148*, 449. [Crossref]
19. Rajabi, M.; Ali, A.; McConnell, M.; Cabral, J.; *Mater. Sci. Eng., C* **2020**, *110*, 110612. [Crossref]
20. Shavandi, A.; Bekhit, A. E. D. A.; Carne, A.; Bekhit, A.; *J. Bioact. Compat. Polym.* **2017**, *32*, 163. [Crossref]
21. Xie, Z.; Zhao, Q.; Wang, H.; Wen, L.; Li, W.; Zhang, X.; Lin, W.; Li, H.; Xie, Q.; Wang, Y.; *Poult. Sci.* **2020**, *99*, 6481. [Crossref]
22. Ramirez, D. O. S.; Carletto, R. A.; Tonetti, C.; Giachet, F. T.; Varesano, A.; Vineis, C.; *Food Packag. Shelf Life* **2017**, *12*, 100. [Crossref]
23. Xu, H.; Shi, Z.; Reddy, N.; Yang, Y.; *J. Agric. Food Chem.* **2014**, *62*, 9145. [Crossref]
24. Majeed. Z.; Farhat, H.; Ahmad, B.; Iqbal, A.; Faiz, A.-ul-H.; Mahnashi, M. H.; Alqarni, A. O.; Alqahtani, O.; Ali, A. A.; Momenah, A. M.; *PeerJ* **2023**, *11*, e15653. [Crossref]
25. Sharma, S.; Gupta, A.; Chik, S. M. S. B. T.; Kee, C. Y. G.; Poddar, P. K.; *IOP Conf. Ser.: Mater. Sci. Eng.* **2017**, *191*, 012013. [Crossref]
26. Zebhi-Ashkezari, V.; Fazaelipoor, M. H.; *Discover Chemistry* **2025**, *2*, 100. [Crossref]
27. Yousif, M.; Cunningham, E.; Smyth, B.; Bolaji, I.; *Waste Biomass Valorization* **2025**. [Crossref]
28. Martínez-Hernández, A. L.; Velasco-Santos, C.; de Icaza, M.; Castaño, V. M.; *Int. J. Environ. Pollut.* **2005**, *23*, 162. [Crossref]
29. Orjuela-Palacio, J. M.; Zaritzky, N. E.; *Ciencia y Tecnología Agropecuaria* **2023**, *24*, 1. [Crossref]
30. Sharma, S.; Gupta, A.; Chik, S. M. S. T.; Kee, C. Y. G.; Podder, P. K.; Subramaniam, M.; Thuraisingam, J.; *IIUM Engineering Journal* **2017**, *18*, 47. [Crossref]
31. Maurya, S. D.; Singh, A.; *Environmental Protection Research* **2023**, *3*, 372. [Crossref]
32. Prajapati, S.; Koirala, S.; Anal, A. K.; *Appl. Biochem. Biotechnol.* **2021**, *193*, 2497. [Crossref]
33. Sharma, S.; Gupta, A.; Chik, S. M. S. T.; Kee, C. Y. G.; Podder, P. K.; Thraisingam, J.; Subramaniam, M.; *The National Conference for Postgraduate Research*; Universiti Malaysia Pahang, Pekan, Malaysia, 2016. [Link] accessed in February 2026
34. Zhou, L. T.; Yang, G.; Yang, X. X.; Cao, Z. J.; Zhou, M. H.; *Environ. Sci. Pollut. Res.* **2014**, *21*, 5730. [Crossref]
35. Rajabinejad, H.; Zoccola, M.; Patrucco, A.; Montarsolo, A.; Rovero, G.; Tonin, C.; *Text. Res. J.* **2018**, *88*, 2415. [Crossref]
36. Ramakrishnan, N.; Sharma, S.; Gupta, A.; Alashwal, B. Y.; *Int. J. Biol. Macromol.* **2018**, *111*, 352. [Crossref]
37. Xing, Y.; Liu, H.; Yu, W.; *J. Mol. Struct.* **2016**, *1106*, 53. [Crossref]
38. Estévez-Martínez, Y.; Velasco-Santos, C.; Martínez-Hernández, A. L.; Delgado, G.; Cuevas-Yáñez, E.; Alaníz-Lumbreras, D.; Castaño, V. M.; *J. Nanomater.* **2013**, *2013*, 702157. [Crossref]
39. Idris, A.; Vijayaraghavan, R.; Patti, A. F.; Macfarlane, D. R.; *ACS Sustainable Chem. Eng.* **2014**, *2*, 1888. [Crossref]
40. Zhang, Y.; Zhao, W.; Yang, R.; *ACS Sustainable Chem. Eng.* **2015**, *3*, 2036. [Crossref]
41. Ma, B.; Qiao, X.; Hou, X.; Yang, Y.; *Int. J. Biol. Macromol.* **2016**, *89*, 614. [Crossref]
42. Alahyaribeik, S.; Ullah, A.; *ChemistrySelect* **2020**, *5*, 13788. [Crossref]
43. Zhu, J.; Mao, N.; *Proceedings of the 14th World Textile Conference*; Bursa, Turkey, 2014. [Link] accessed in February 2026
44. Brebu, M.; Spiridon, I.; *J. Anal. Appl. Pyrolysis* **2011**, *91*, 288. [Crossref]
45. Valkov, A.; Zinigrad, M.; Sobolev, A.; Nisnevitch, M.; *Int. J. Mol. Sci.* **2020**, *21*, 3512. [Crossref]
46. Poole, A. J.; Church, J. S.; *Int. J. Biol. Macromol.* **2015**, *73*, 99. [Crossref]
47. Qin, X.; Yang, C.; Guo, Y.; Liu, J.; Bitter, J. H.; Scott, E. L.; Zhang, C.; *Ultrason. Sonochem.* **2023**, *93*, 106297. [Crossref]

48. Aluigi, A.; Zoccola, M.; Vineis, C.; Tonin, C.; Ferrero, F.; Canetti, M.; *Int. J. Biol. Macromol.* **2007**, *41*, 266. [Crossref]
49. Mi, X.; Li, W.; Xu, H.; Mu, B.; Chang, Y.; Yang, Y.; *Waste Manage.* **2020**, *115*, 65. [Crossref]
50. Sharma, S.; Gupta, A.; Kumar, A.; Kee, C. G.; Kamyab, H.; Saufi, S. M.; *Clean Technol. Environ. Policy* **2018**, *20*, 2157. [Crossref]
51. Wu, M.; Shen, S.; Yang, X.; Tang, R.; *IOP Conf. Ser.: Mater. Sci. Eng.* **2017**, *254*, 042030. [Crossref]
52. Jafari, M.; Mehrnejad, F.; Rahimi, F.; Asghari, S. M.; *Sci. Rep.* **2018**, *8*, 2150. [Crossref]
53. Schrooyen, P. M. M.; Dijkstra, P. J.; Oberthür, R. C.; Bantjes, A.; Feijen, J.; *J. Colloid Interface Sci.* **2001**, *240*, 30. [Crossref]
54. Fernández-d'Arlas, B.; Peña-Rodríguez, C.; Eceiza, A.; *Revista Iberoamericana de Polímeros* **2016**, *17*, 110. [Link] accessed in February 2026
55. Misra, M.; Kar, P.; Priyadarshan, G.; Licata, C.; *MRS Online Proc. Libr.* **2002**, *702*, 35. [Crossref]
56. Shavandi, A.; Silva, T. H.; Bekhit, A. A.; Bekhit, A. E. D. A.; *Biomater. Sci.* **2017**, *5*, 1699. [Crossref]
57. Viitala, J.; Lappalainen, T.; Järvinen, M.; *Nord. Pulp Pap. Res. J.* **2020**, *35*, 261. [Crossref]
58. Poole, A. J.; Church, J. S.; Huson, M. G.; *Biomacromolecules* **2009**, *10*, 1. [Crossref]
59. Nakata, R.; Osumi, Y.; Miyagawa, S.; Tachibana, A.; Tanabe, T.; *J. Biosci. Bioeng.* **2015**, *120*, 111. [Crossref]
60. Wang, J.; Hao, S.; Luo, T.; Yang, Q.; Wang, B.; *Mater. Sci. Eng., C* **2016**, *68*, 768. [Crossref]
61. Li, W.; Gao, F.; Kan, J.; Deng, J.; Wang, B.; Hao, S.; *Colloids Surf., B* **2019**, *175*, 436. [Crossref]
62. Du, J.; Wu, Q.; Li, Y.; Liu, P.; Han, X.; Wang, L.; Xiao, Y.; *J. Biomater. Sci., Polym. Ed.* **2020**, *31*, 1163. [Crossref]
63. Azarniya, A.; Tamjid, E.; Eslahi, N.; Simchi, A.; *Int. J. Biol. Macromol.* **2019**, *134*, 280. [Crossref]
64. Nei, D.; Okunishi, T.; *Journal of the NARO Research and Development* **2022**, *10*, 47. [Crossref]